Science Advances
AAAS

advances.sciencemag.org/cgi/content/full/5/8/eaaw8357/DC1

Supplementary Materials for

Noninvasive monitoring of chronic kidney disease using pH and perfusion imaging

KowsalyaDevi Pavuluri, Irini Manoli, Alexandra Pass, Yuguo Li, Hilary J. Vernon, Charles P. Venditti, Michael T. McMahon*

*Corresponding author. Email: mcmahon@kennedykrieger.org

Published 14 August 2019, *Sci. Adv.* **5**, eaaw8357 (2019)
DOI: 10.1126/sciadv.aaw8357

This PDF file includes:

Supplementary Figures

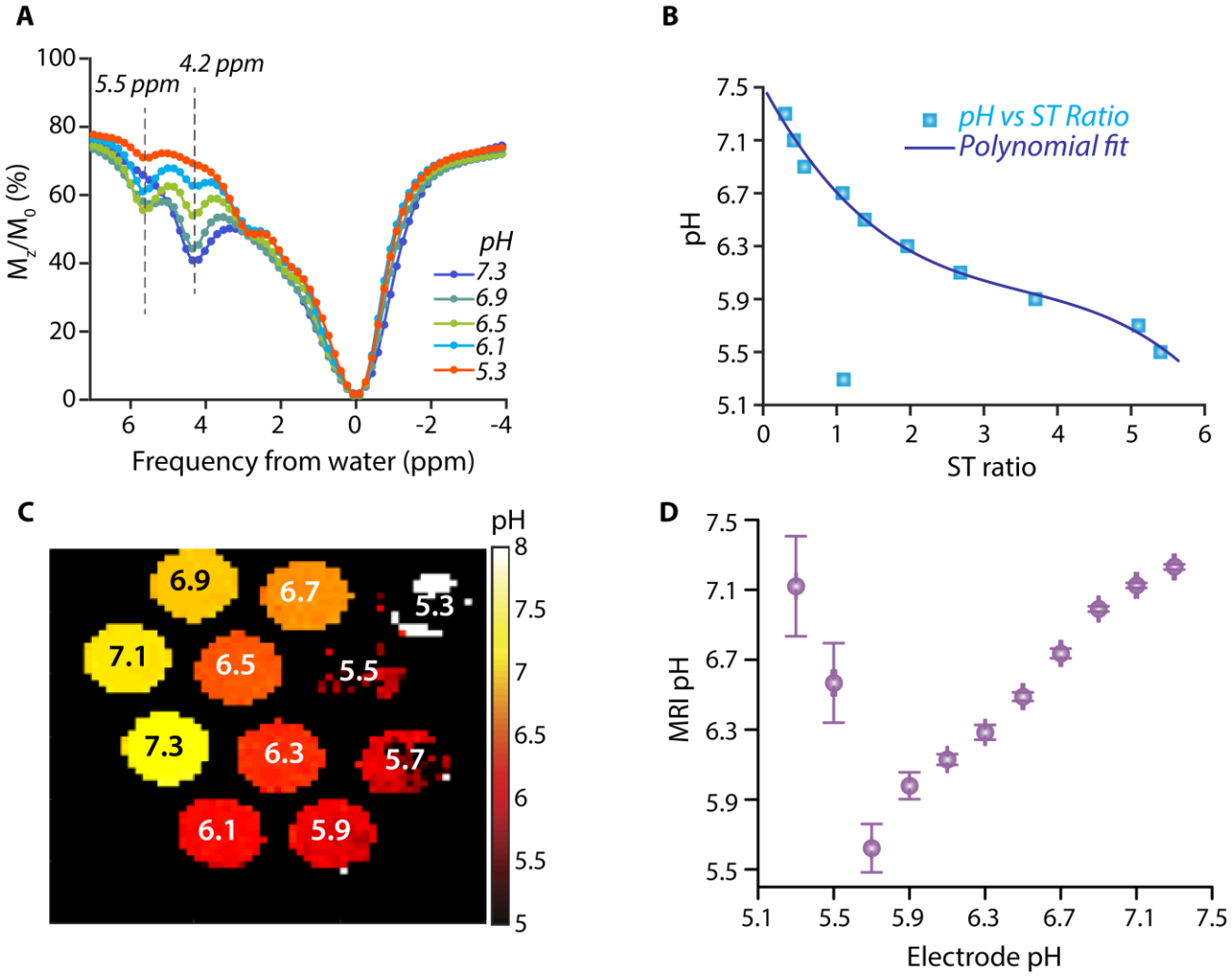

Fig. S1. In vitro results at RF saturation field strength of 3 μT. (**A**) CEST z-spectra of iopamidol in blood serum at ω_1 = 3 μT for pH = 5.3, 6.1, 6.5, 6.9 and 7.3; (**B**) Calibration plot used to calculate in vitro and in vivo pH, variation of experimental ST ratio at different pH values was given by $pH = p_1 \times (\text{ST ratio})^3 + p_2 \times (\text{ST ratio})^2 + p_3 \times (\text{ST ratio})^1 + p4$; where $p_1 = -0.0237$; $p_2 = 0.2509$; $p_3 = -1.029$; $p_4 = 7.508$; RMSE = 0.065. pH values from 5.5 to 7.3 were considered for the polynomial fit. (**C**) pH maps of iopamidol-serum phantom. In the map pH values below 5.7 were determined inaccurately. (**E**) Error bar plots representing the accuracy in MRI pH measurements compared to that of electrode pH for iopamidol-serum phantom. Error bars were obtained by calculating the mean standard deviation in pH over an ROI drawn enclosing each entire tube in the phantom.

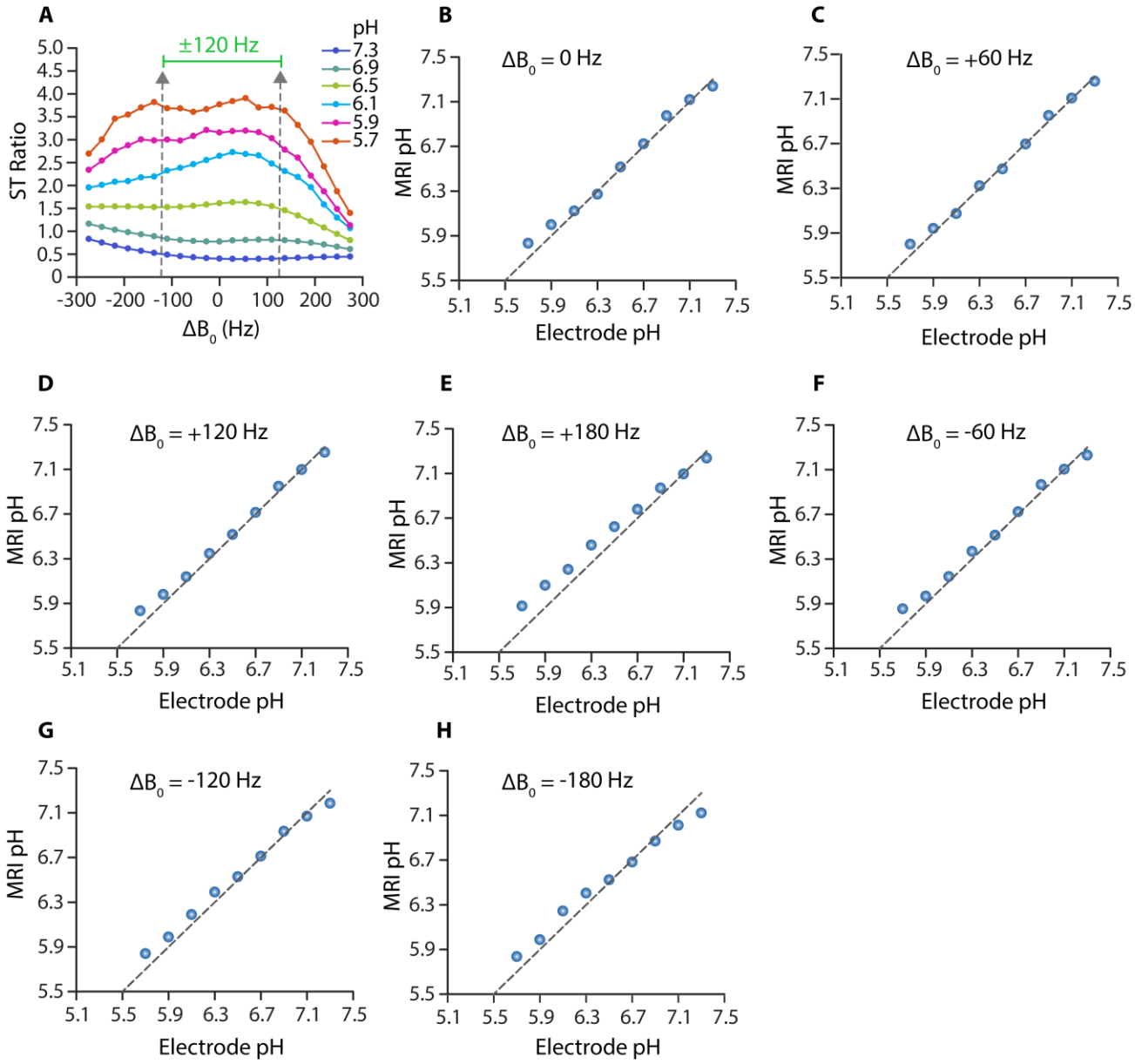

Fig. S2. In vitro pH measurement variation as a function of ΔB_0 shift at 4-μT RF saturation power. (**A**) ST ratio vs ΔB_0 for pH values between 5.7 and 7.3. ΔB_0 with ±120 Hz are highlighted using vertical gray lines because field differences less than these were shown to produce errors < 0.1 pH unit for all pH values from 5.7 to 7.3; A ΔB_0 of +180 Hz impacts pH calculations with 5.7 and 5.9 producing errors of 0.2 and 0.1 pH units respectively. (**B**), (**C**), (**D**), (**E**), (**F**), (**G**) and (**H**) are the MRI pH values calculated at ΔB_0 = 0, +60, +120, +180, -60, -120 and -180 Hz respectively with the dashed black line representing perfect agreement.

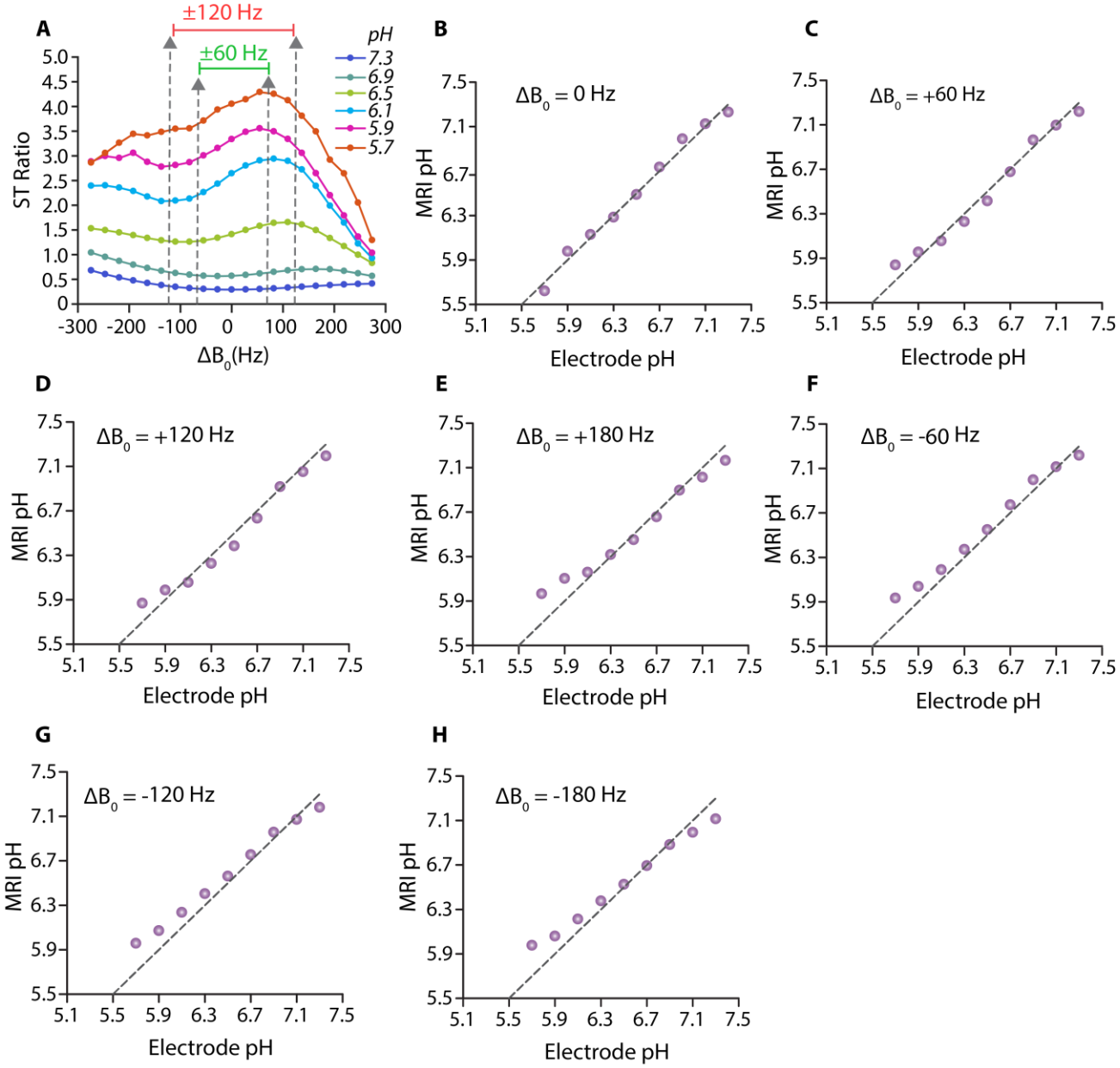

Fig. S3. In vitro pH measurement variation with ΔB_0 shift at 3-μT RF saturation power. (**A**) ST ratio vs ΔB_0 for pH values between 5.7 and 7.3. ΔB_0 of less than ±60 Hz Hz are highlighted using vertical gray lines because field differences less than these were shown to produce errors <0.1 pH unit for all pH values between 5.7 and 7.3. ΔB_0 of greater than ±60 Hz produces errors of 0.2 and 0.1 pH units for pH values 5.7 ad 7.3. (**B**), (**C**), (**D**), (**E**), (**F**), (**G**) and (**H**) are the MRI pH values calculated at ΔB_0 = 0, +60, +120, +180, -60, -120 and -180 Hz respectively with the dashed gray line representing perfect agreement.

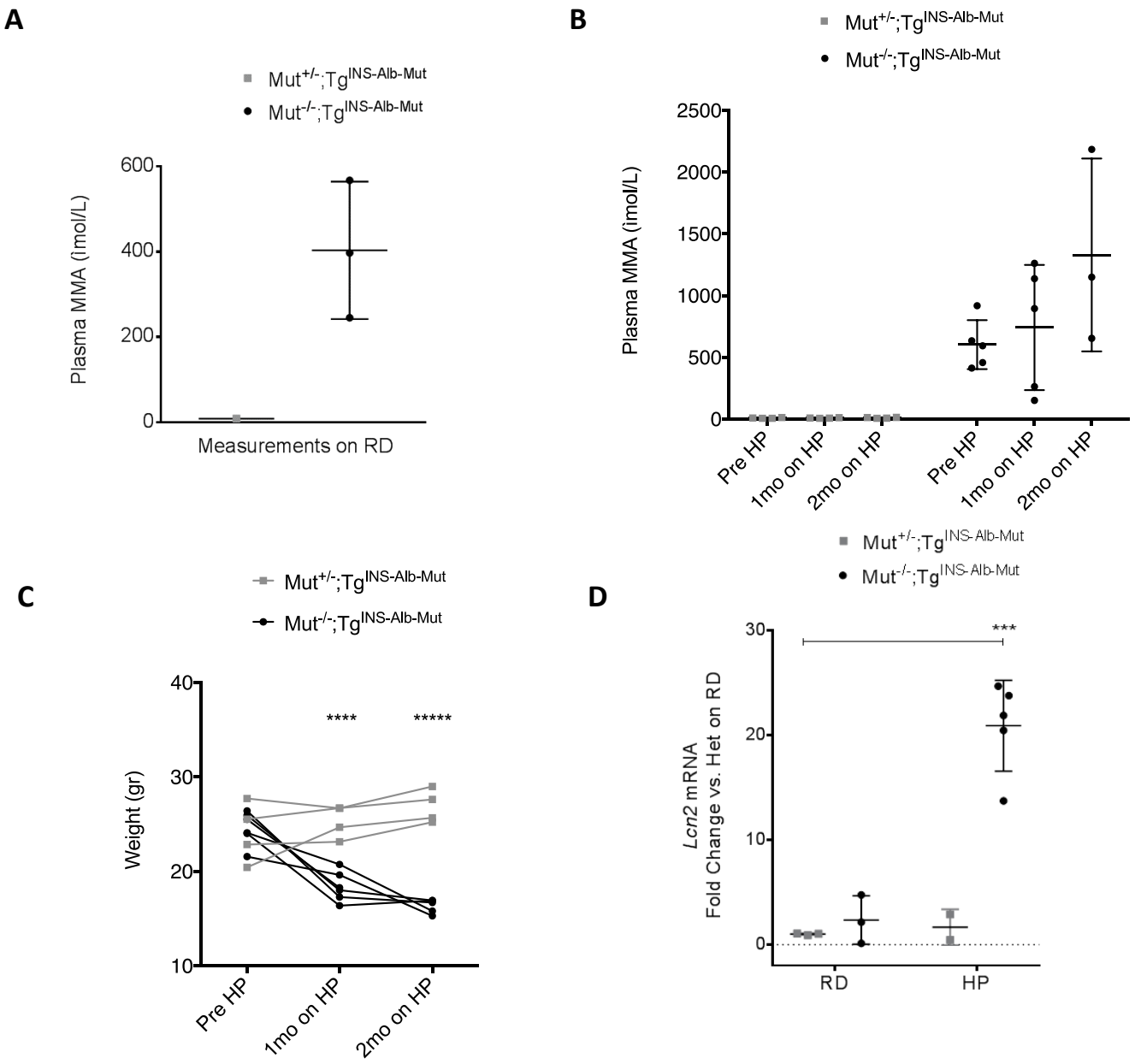

Fig. S4. Biochemical and clinical measures in the RD and HP *Mut*$^{-/-}$;Tg$^{\text{INS-Alb-Mut}}$ mice as compared to heterozygote littermates. (**A**) Plasma methylmalonic acid concentrations (μmol/L) in unchallenged mice on regular chow (N = 4 and 1 for Mut$^{-/-}$; Tg$^{\text{INS-Alb-Mut}}$ and heterozygote control). (**B**) Plasma methylmalonic acid concentrations (μmol/L) over time in mice on high protein diet (N = 3-5 mutant and 4 heterozygote animals, P<0.05 for all time points, two mutant mice died during the diet challenge study).(**C**) Body weight (grams) of the animals during the high protein challenge (P<0.0001 at the 1 and 2 month time points). (**D**) Kidney Lcn2 (Lipocalin-2) mRNA expression differences between mutant mice on regular chow or high protein diet, expressed as fold change compared to the unchallenged heterozygote mice on RD (P=0.0021 for mutant mice on HP compared to heterozygote mice on RD).

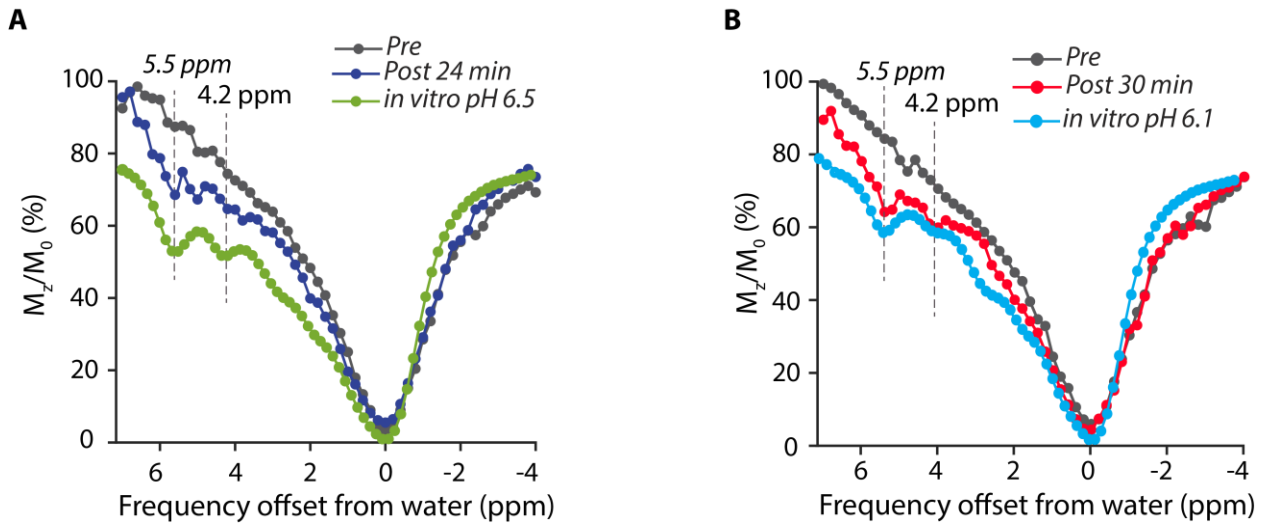

Fig. S5. In vivo Z-spectra. (**A**) Z-spectrum for preinjection data of $Mut^{+/-}$ healthy control (dark grey), post injection z-spectrum (dark blue) and invitro z-spectrum of pH 6.5 for iopamidol in serum phantom (dark green). (**B**) Preinjection Z-spectrum of RD $Mut^{-/-}$ (dark grey), postinjection z-spectrum (red) and in vitro z-spectrum (light blue).

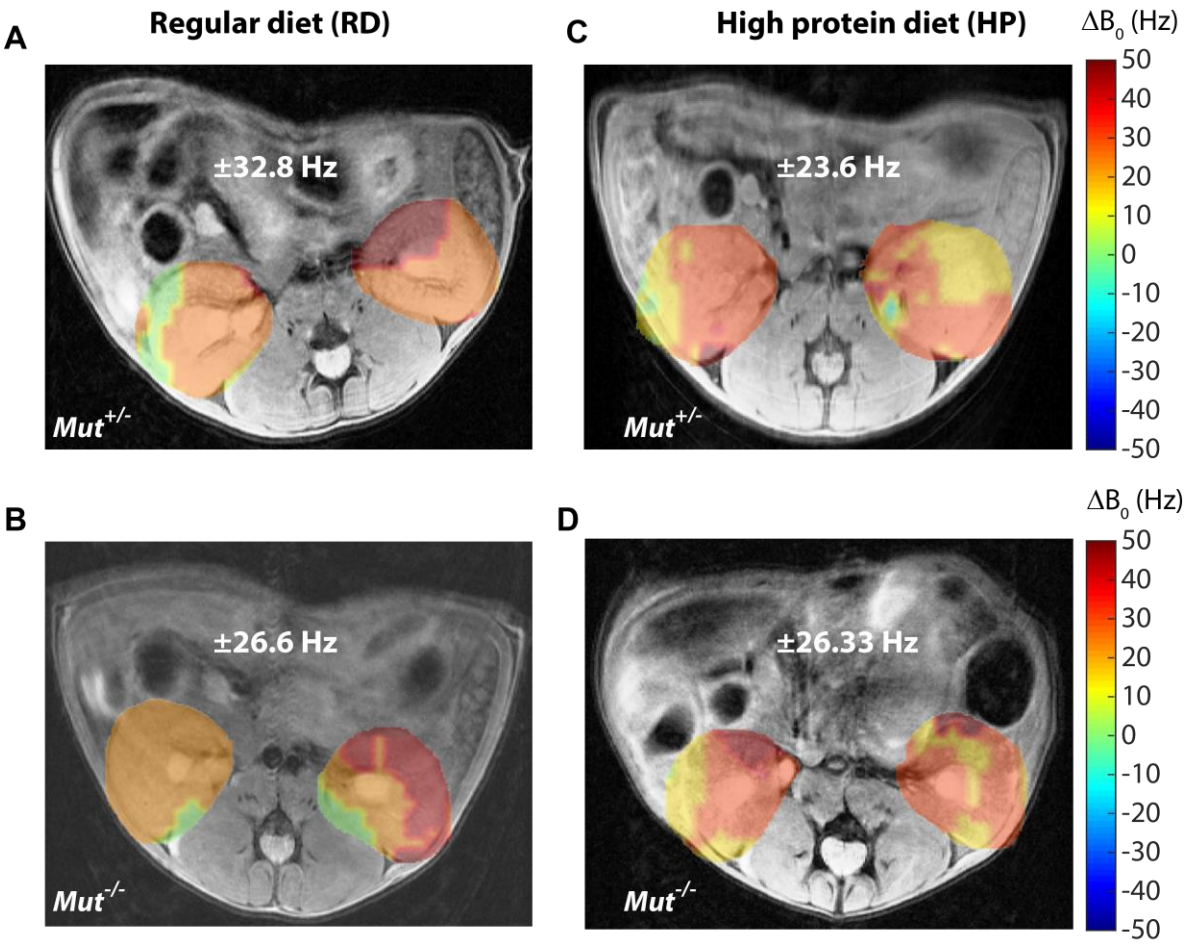

Fig. S6. Representative ΔB_0 maps for RD and HP diet mice. ΔB_0 are generated using WASSR experiment performed using 0.5 μT RF saturation power and 42 offsets between +1.5 ppm and -1.5 ppm. The mean frequency shift in water frequency and the standard deviation was mentioned in the image. (**A**), (**B**) $Mut^{+/-}$ and $Mut^{-/-}$ mice of regular diet mice. (**C**), (**D**) $Mut^{+/-}$ and $Mut^{-/-}$ of high protein diet mice.

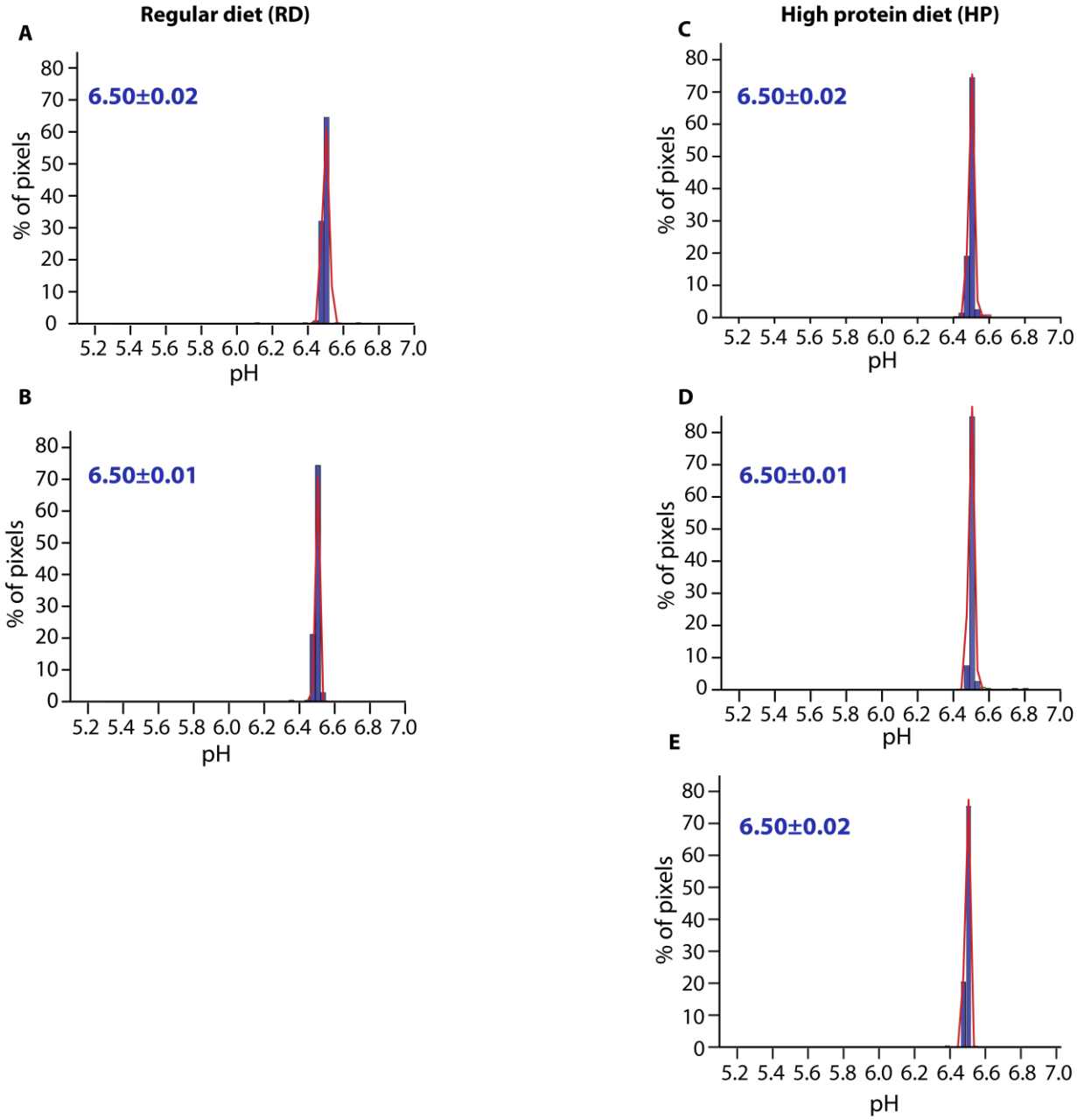

Fig. S7. pH-histogram plots depicting the percentage of pixels across the detectable pH range and normal distribution analysis for all control (*Mut*$^{+/-}$) mice imaged in this study. The percentage of pixels were calculated by drawing an ROI over both kidneys. A gaussian distribution was assumed to estimate the pH range over both kidneys in the imaging slice. Weights of the mice were 24, 27, 23, 23, 23 g respectively. The mean pH value and pH range at half height are indicated in the figure legend for each mouse. (**A**), (**B**) (**C**), (**D**) and (**E**) are the pH histogram distributions of Mut$^{+/-}$ of RD and HP diet groups. 75-80 % of the pixels in both kidneys of healthy controls are shown mean pH at 6.50 with a very narrow distribution range less than 0.02.

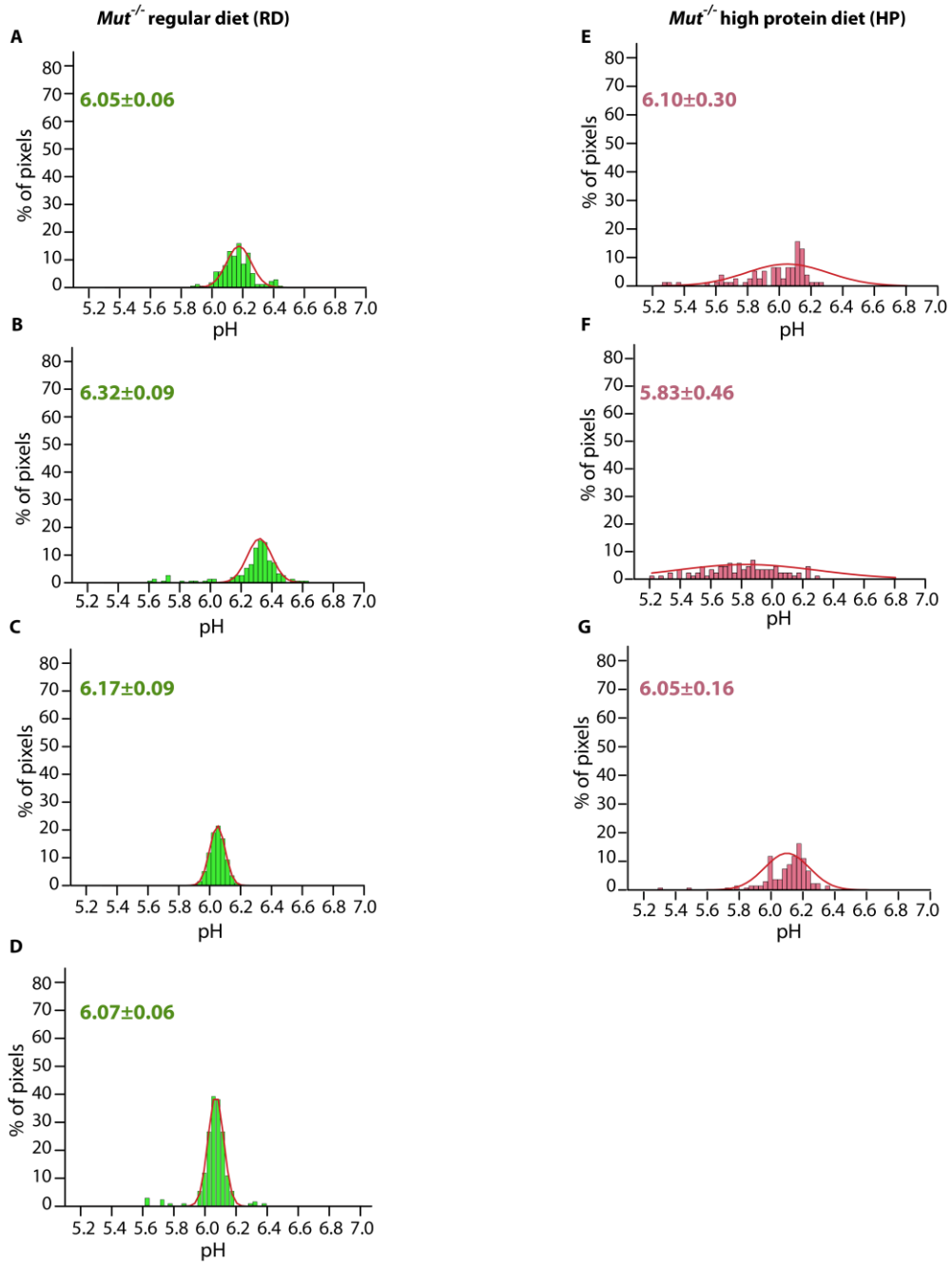

Fig. S8. pH-histogram plots depicting the percentage of pixels across the detectable pH range and normal distribution analysis for all *Mut*$^{-/-}$ mice imaged in this study. (**A**), (**B**), (**C**) and (**D**) are the histogram distributions of RD Mut$^{-/-}$ mice. The weights of these mice were 28, 24, 30 and 28 g respectively. The mean pH reduces to 6.05-6.32 and pH distribution expands to 0.06-0.09 in these mice. (E), (F) and (G) are the pH-histograms of HP Mut$^{-/-}$ mice. Weights of these mice were 16, 15 and 19 g respectively. The mean pH reduced to a minimum of 5.83. pH over the pixels and the range in pH values expanded to 0.16-0.46.

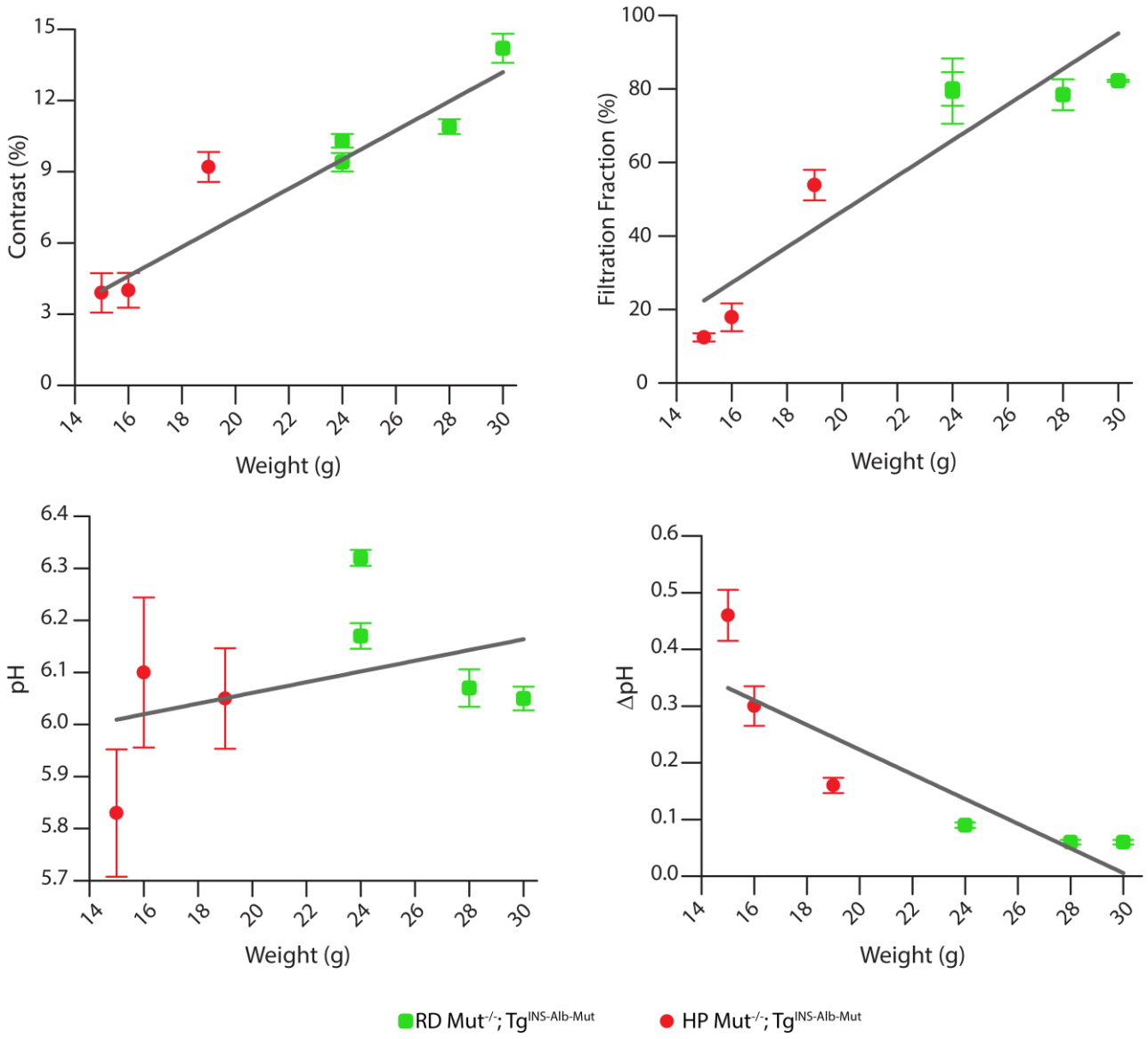

Fig. S9. MRI metrics versus weight correlation plots for HP and RD *Mut*$^{-/-}$ mice. (A) Maximum image contrast vs. weight correlation plot for RD and HP Mut$^{-/-}$ mice with R = 0.93; (B) Filtration fraction vs. weight correlation plot for RD and HP Mut$^{-/}$ mice with R = 0.9; (C) pH vs. weight correlation plot for RD and HP Mut$^{-/-}$ mice. The correlation coefficient was substantially lower than for other MRI metrics with R = 0.0624. (D) ΔpH vs. weight correlation plot with R=0.85.

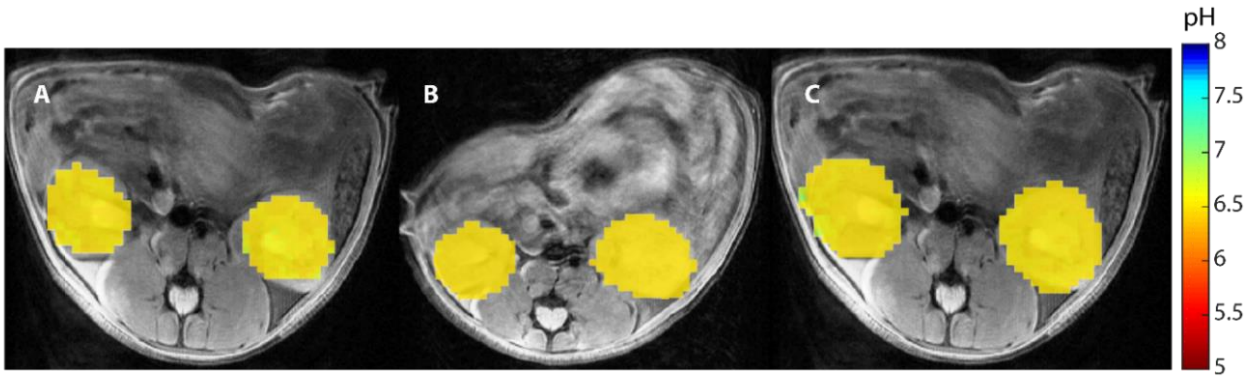

Fig. S10. pH images calculated for a healthy control mouse using our 72, 38, and 2-offset protocols. pH images calculated for a healthy control mouse using our (A) 72, (B) 38, and (C) 2 offset protocols at 40 min post iopamidol administration. The mean renal pH in these images was 6.5, showing the robustness of our protocol and processing.